Front. Electr. Electron. Eng. China (2006) 2: 171–176
DOI 10.1007/s 11460-006-0001-8

RESEARCH ARTICLE

**DU Lan, LIU Hong-wei, BAO Zheng, ZHANG Jun-ying**

# A new feature extraction method using the amplitude fluctuation property of target HRRP for radar automatic target recognition



**Abstract** Due to the aspect sensitivity of high-resolution range profile (HRRP), traditional radar HRRP target recognition methods usually use average profile within some target-aspect region as the target-aspect template. Actually, the amplitude fluctuation property of target HRRP also represents some feature information of the target. Based on the scattering center model, a new feature extraction method using the amplitude fluctuation property of target HRRP is proposed in this paper. The weighted HRRP feature extracted by the new method can represent the scatterer distribution in every range cell, thereby it can describe the scattering property of the target better. The experimental results based on measured data show that the new feature extraction method can greatly improve recognition performances.

**Keywords** Radar automatic target recognition (RATR), HRRP, Feature extraction, Scattering center model, Average profile, Variance profile

## 1 Introduction

A high-resolution range profile (HRRP) represents the projection of the complex returned echoes from target scattering centers onto the radar line-of-sight (LOS). It contains the target structure signatures, such as target size, scatterer distribution, etc.. Radar HRRP target recognition has received much attention from the RATR community [1–7]. However, according to the scattering center model [8–9], which is widely used by the high range resolution radar imaging community (SAR/ISAR), the variation of target-aspect will lead to different range shifts for different scattering centers on the target. Therefore, the HRRP, the amplitude of coherent sum of the complex returned echoes from scatterers in a range resolution cell, can be changed substantially. This is referred to as the target-aspect sensitivity of HRRP. Thus, the traditional radar HRRP target recognition methods usually use an average profile within some target-aspect region as the target-aspect template [2–6], such as template matching method under the maximum correlation coefficient criterion (MCC-TMM) [1, 4, 6], namely, minimum Euclidean distance classifier, and some kernel function classifiers [6]. Actually, the amplitude fluctuation property of target HRRP also represents some feature information of the target [1]. On the assumption that target data are distributed as multivariate Gaussian, adaptive Gaussian classifier (AGC) uses Bayesian theory to minimize cost function. Because using variance matrix of target HRRP can reflect its amplitude fluctuation property, AGC outperforms MCC-TMM in radar HRRP target recognition [7]. Nevertheless, if test data are mismatched with the distribution model estimated from training data or if the parameters of the distribution model are not estimated exactly, the recognition performance of AGC will degrade.

This paper proposes a new feature extraction method different from AGC, which describes HRRP's statistical characteristics using the amplitude fluctuation property of target HRRP according to the scattering center model. The weighted HRRP feature extracted by the new method, which effectively fuses the average profile with the variance profile of an HRRP frame, can represent the scatterer distribution in every range cell. Therefore, it can describe the scattering property of the target better. Furthermore, in order to deal with the amplitude-scale and time-shift sensitivity of target HRRP, a joint amplitude-shift matching fast algorithm is proposed in this paper, which can reduce the computation burden effectively. By using this fast algorithm, the weighted HRRP feature can be used in any classifier based on Euclidean distance. In recognition experiments based on measured data, the MCC-TMM and

Translated from *Acta Electronica Sinica,* 2005, 33(3): 411-415 (in Chinese)

DU Lan (✉), LIU Hong-wei, BAO Zheng, ZHANG Jun-ying
National Laboratory of Radar Signal Processing, Xidian University, Xi'an, Shaanxi 710071, China

the radial basis function network (RBFN) using the proposed weighted HRRP feature achieve better recognition performances than those using the traditional average profile template and AGC which also uses amplitude fluctuation property of target HRRP.

## 2 Scattering center model-based property analysis and feature extraction of target HRRP

### 2.1 Property analysis based on scattering center model

According to the scattering center model [8–9], the limitation of target-aspect change for avoiding scatterers' motion through range cells (MTRC) is given by

$$\delta\varphi \le (\delta\varphi)_{\mathrm{MTRC}} = \frac{\Delta R}{L} \tag{1}$$

where $\Delta R$ is the length of range cell and $L$ is the cross length of target. Since the scattering center model almost remains unchanged within $\Delta\varphi$, the HRRPs in this sector can be regarded as a vector stationary process. Thus, HRRPs of one target can be divided into many subsets according to different angular sectors, which are defined as HRRP frames in this paper. According to relevant literatures [2–6], an HRRP consists of the scatterer auto-term (SAT) and the scatterer cross-term (SCT). If a target uniformly rotates within the target-aspect sector corresponding to an HRRP frame, the power of the $m$th returned echo ($m = 0, 1, \cdots, M-1$) in the $n$th range cell ($n = 1, 2, \cdots, N$) can be written as

$$|x_n(m)|^2 = \sum_{i=1}^{L_n}\sigma_{ni}^2 + 2\sum_{i=2}^{L_n}\sum_{k=1}^{i-1}\sigma_i\sigma_k\cos[\theta_{nik}(m)] \tag{2}$$

where $\sigma_{ni}$ represents the strength of the $i$th scatterer, $\theta_{nik}(m)$ represents the phase difference between the $i$th scatterer and the $k$th scatterer of the $m$th echo in the $n$th range cell. The first term at the right side of Eq. (2) is referred to as the SAT, which is the summation of the scatterers' energy within a range cell; the second term is referred to as the SCT, which is the summation of conjugate multiplication of echoes from different scatterers within a range cell. Without MTRC, the SAT remains invariant, but the SCT varies as a random variable with zero mean [2–6]. Thus, the target-aspect sensitivity of HRRP results from the SCT. Therefore, as far as a range cell is concerned, the mean of $\left\{|x_n(0)|^2, |x_n(1)|^2, \cdots, |x_n(M-1)|^2\right\}$ can represent the stable SAT approximately, and the variance can represent the fluctuation property of the SCT.

According to the scattering center model, there are three kinds of scatterer distributions in a range cell [9].

1) First type of range cell: there are a large number of small scatterers and no predominant scatterers in this type of range cell. Under the hypothesis that the strengths of the small scatterers are almost the same and the number of the small scatterers is large enough, the amplitude of this type of range cell will follow a Rayleigh distribution and slightly fluctuate.

2) Second type of range cell: this type of range cell consists of a predominant scatterer and a large number of small scatterers. Under the hypothesis similar to the first type, the amplitude of this type of range cell will follow a Ricean distribution and mainly depend on the dominant scatterer with slight fluctuation caused by small scatterers.

3) Third type of range cell: there are a large number of small scatterers and several predominant scatterers in this type of range cell. Due to the difference in range-shifts between dominant scatterers, the amplitude of this type of range cell will follow a multimodal (mainly bimodal) distribution, which depends on the particular geometrical distribution of the dominant scatterers, and have great fluctuation along with target aspect changing.

### 2.2 A new feature extraction method

In order to deal with the target-aspect sensitivity of HRRP, the traditional radar HRRP target recognition methods usually use the average profile of each HRRP frame as the target-aspect template and a single HRRP sample as a test sample [2–6]. As discussed in Sect. 2.1, the average profile can approximately represent the stable SATs of all range cells within an HRRP frame. Nevertheless, with different scatterer distributions, range cells of a test HRRP have different amplitude fluctuation properties, of which some are stable and some have great fluctuation. In radar HRRP target recognition, stable range cells are more important than unstable ones. Therefore, if HRRP components are multiplied by different weights that depend on their amplitude fluctuation property, the recognition performance will be improved.

Let $\boldsymbol{\mu}_{ik} = [\mu_{ik}(1), \mu_{ik}(2), \cdots, \mu_{ik}(N)]^{\mathrm{T}}$, $\boldsymbol{c}_{ik} = \left[\sigma_{ik}^2(1), \sigma_{ik}^2(2), \cdots, \sigma_{ik}^2(N)\right]^{\mathrm{T}}$ respectively represent the average profile and variance profile of the $k$th HRRP frame $\{\boldsymbol{x}_{ikl} \mid l = 1, 2, \cdots, L\}$ of $i$th target ($L$ denotes the sample number), and let $\left[n_1, n_{S_{ik}}\right]$ denote the signal support region of $\boldsymbol{\mu}_{ik}$, in other words, noises distribute out of $\left[n_1, n_{S_{ik}}\right]$. The weight vector of $\{\boldsymbol{x}_{ikl} \mid l = 1, 2, \cdots, L\}$ is defined as

$$\boldsymbol{w}_{ik} \triangleq \left[0, 0, \cdots, \frac{1}{\sigma_{ik}(n_1)}, \frac{1}{\sigma_{ik}(n_2)}, \cdots, \frac{1}{\sigma_{ik}(n_{S_{ik}})}, 0, 0, \cdots, 0\right]^{\mathrm{T}} \tag{3}$$

The corresponding feature template is

$$\boldsymbol{v}_{ik} = \boldsymbol{\mu}_{ik} \cdot \boldsymbol{w}_{ik} = \left[0, 0, \cdots, \frac{\mu_{ik}(n_1)}{\sigma_{ik}(n_1)}, \frac{\mu_{ik}(n_2)}{\sigma_{ik}(n_2)}, \cdots, \frac{\mu_{ik}(n_{S_{ik}})}{\sigma_{ik}(n_{S_{ik}})}, 0, 0, \cdots, 0\right]^{\mathrm{T}} \tag{4}$$

When a test profile $\boldsymbol{x} = [x(1), x(2), \cdots, x(N)]^{\mathrm{T}}$ matches with $\{\boldsymbol{x}_{ikl} \mid l = 1, 2, \cdots, L\}$, $\boldsymbol{x}$ is assumed to have the same scatterer distribution as $\{\boldsymbol{x}_{ikl} \mid l = 1, 2, \cdots, L\}$. Therefore, the

test feature vector is

$$\boldsymbol{\chi}_{ik} = \boldsymbol{x}\boldsymbol{w}_{ik} = \left[0,0,\cdots,0,\frac{x(n_1)}{\sigma_{ik}(n_1)},\frac{x(n_2)}{\sigma_{ik}(n_2)},\cdots,\frac{x(n_{S_{ik}})}{\sigma_{ik}(n_{S_{ik}})},0,0,\cdots,0\right]^{\mathrm{T}} \quad (5)$$

The feature vectors defined in Eqs. (4) and (5) reflect not only the absolute amplitude, but also the scatterer distribution of the average profile template and test sample, respectively. Thus, they can describe the scattering property of the target better.

## 3 RATR based on weighted HRRP feature

### 3.1 Amplitude-scale and time-shift sensitivity

Radar HRRP is also sensitive to amplitude-scale and time-shift variations [4, 6]. In radar HRRP target recognition, firstly, the test samples and target-aspect templates should be amplitude-scale normalized, e.g., $L_2$ normalization [4, 6]; secondly, the amplitude-scale normalized test samples should be time-shift matched with the amplitude-scale normalized target-aspect templates [4, 6]. When our feature extraction method is used, the matching process between a test feature vector and a feature template is shown in Fig. 1, which comes from the measured data of "Yark-42" (detailed introduction shown in Sect. 4.1). Since the weight vector defined in Eq. (4) is time-shift matched with the average profile template but not with the test sample, the amplitude-scales of the test sample with different time-shift compensations are also different. Therefore, as shown in Fig. 1, the amplitude-scale normalization should be done along with the time-shift compensation. However, such matching process will mean a huge computation burden. In order to reduce computation burden, a joint amplitude-shift matching fast algorithm is proposed as follows.

### 3.2 Joint amplitude-shift matching fast algorithm

Let $\overline{\boldsymbol{v}}_{ik} = \boldsymbol{v}_{ik} / \|\boldsymbol{v}_{ik}\|_2$ denote the normalized feature template of the $k$th HRRP frame of $i$th target, and let $\overline{\boldsymbol{\chi}}_{ik\tau} = \boldsymbol{\chi}_{ik\tau} / \|\boldsymbol{\chi}_{ik\tau}\|_2$ represent the normalized test feature vector with time-shift $\tau$, where

$$\boldsymbol{\chi}_{ik\tau} = \boldsymbol{x}_\tau \cdot \boldsymbol{w}_{ik} = \left[x((1+\tau))_N w_{ik}(1), x((2+\tau))_N w_{ik}(2), \cdots, x((N+\tau))_N w_{ik}(N)\right]^{\mathrm{T}} \quad (6)$$

and $x((n+\tau))_N$ denotes the $n$th component of test profile $\boldsymbol{x}$ with circular time shift $\tau$. The square Euclidean distance between $\overline{\boldsymbol{\chi}}_{ik\tau}$ and $\overline{\boldsymbol{v}}_{ik}$ is

$$d^2_{\mathrm{E}|ik\tau} = \left(\overline{\boldsymbol{\chi}}_{ik\tau} - \overline{\boldsymbol{v}}_{ik}\right)^{\mathrm{T}}\left(\overline{\boldsymbol{\chi}}_{ik\tau} - \overline{\boldsymbol{v}}_{ik}\right) = 2 - 2\overline{\boldsymbol{\chi}}^{\mathrm{T}}_{ik\tau}\overline{\boldsymbol{v}}_{ik} = 2 - 2\rho(\boldsymbol{\chi}_{ik\tau}, \boldsymbol{v}_{ik}) \quad (7)$$

where $\rho(\boldsymbol{\chi}_{ik\tau}, \boldsymbol{v}_{ik})$ is the cross-correlation coefficient

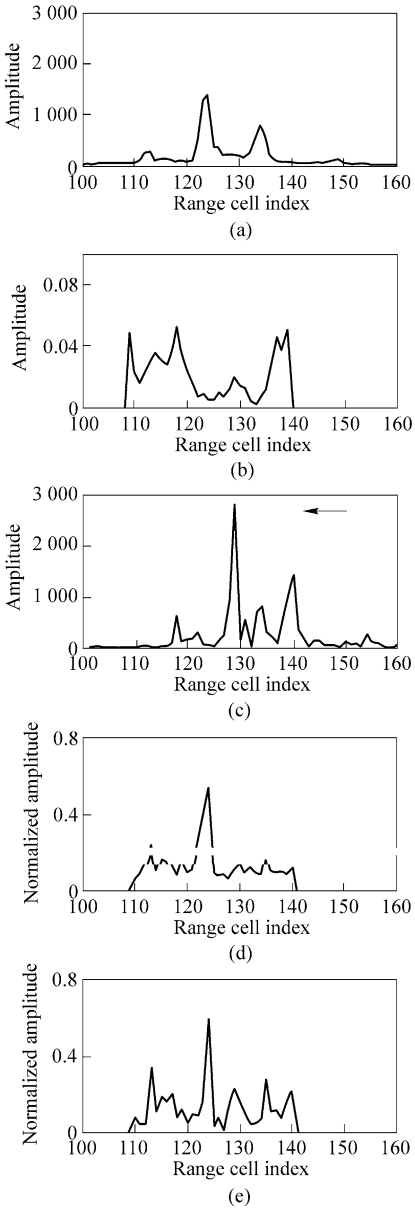


**Fig. 1** Matching process between a test profile and an aspect template. (a) Average profile template; (b) Weight vector; (c) Test sample; (d) Normalized feature template; (e) Normalized test feature vector with time-shift compensation

between $\boldsymbol{\chi}_{ik\tau}$ and $\boldsymbol{v}_{ik}$,

$$\rho(\boldsymbol{\chi}_{ik\tau}, \boldsymbol{v}_{ik}) = \frac{\boldsymbol{\chi}^{\mathrm{T}}_{ik\tau}\boldsymbol{v}_{ik}}{\|\boldsymbol{\chi}_{ik\tau}\|_2 \cdot \|\boldsymbol{v}_{ik}\|_2} = \frac{\sum_{n=1}^{N}\left[x((n+\tau))_N \cdot \left(\overline{v}_{ik}(n) \cdot w_{ik}(n)\right)\right]}{\sqrt{\sum_{n=1}^{N}\left[x^2((n+\tau))_N \cdot w^2_{ik}(n)\right]}} = \frac{\boldsymbol{x}^{\mathrm{T}}_\tau \overline{\boldsymbol{v}}_{ik}}{\sqrt{\hat{\boldsymbol{x}}^{\mathrm{T}}_\tau \hat{\boldsymbol{w}}_{ik}}} \quad (8)$$

with $\hat{x}, \hat{w}_{ik}$ and $\overline{v}_{ik}$ being defined as

$$\hat{\boldsymbol{x}} \triangleq \boldsymbol{x}\cdot\boldsymbol{x}=\left[x^2(1),x^2(2),\cdots,x^2(N)\right]^{\mathrm{T}} \tag{9}$$

$$\hat{\boldsymbol{w}}_{ik} \triangleq \boldsymbol{w}_{ik}\cdot\boldsymbol{w}_{ik}=\left[w_{ik}^2(1),w_{ik}^2(2),\cdots,w_{ik}^2(N)\right]^{\mathrm{T}} \tag{10}$$

$$\begin{aligned}\overline{\boldsymbol{v}}_{ik} &\triangleq \overline{\boldsymbol{v}}_{ik}\cdot\boldsymbol{w}_{ik}\\ &=\left[\frac{v_{ik}(1)w_{ik}(1)}{\|\boldsymbol{v}_{ik}\|_2},\frac{v_{ik}(2)w_{ik}(2)}{\|\boldsymbol{v}_{ik}\|_2},\cdots,\frac{v_{ik}(N)w_{ik}(N)}{\|\boldsymbol{v}_{ik}\|_2}\right]^{\mathrm{T}}\end{aligned} \tag{11}$$

The joint amplitude-shift matching result is

$$d_{\mathrm{E}|ik}=\min_{\tau}\left\{d_{\mathrm{E}|ik\tau}\right\}=\sqrt{2-2\max_{\tau}\left\{\rho(\boldsymbol{\chi}_{ik\tau},\boldsymbol{v}_{ik})\right\}} \tag{12}$$

If using fast Fourier transformation (FFT) and inverse fast Fourier transformation (IFFT) to reduce computation burden, then

$$\begin{aligned}\max_{\tau}\rho(\boldsymbol{\chi}_{ik\tau},\boldsymbol{v}_{ik}) &= \max_{m}\left\{\frac{\mathrm{IFFT}\left[\mathrm{FFT}(\boldsymbol{x})\cdot\mathrm{FFT}(\overline{\boldsymbol{v}}_{ik})\right]}{\sqrt{\mathrm{IFFT}\left[\mathrm{FFT}(\hat{\boldsymbol{x}})\cdot\mathrm{FFT}(\hat{\boldsymbol{w}}_{ik})\right]}}\right\}\\ &= \max_{m}\left\{\frac{r_{\boldsymbol{x},\overline{\boldsymbol{v}}_{ik}}(m)}{\sqrt{r_{\hat{\boldsymbol{x}},\hat{\boldsymbol{w}}_{ik}}(m)}}\right\}\\ m&=1,2,\cdots,N\end{aligned} \tag{13}$$

where

$$\begin{aligned}\boldsymbol{r}_{\boldsymbol{x},\overline{\boldsymbol{v}}_{ik}} &= \boldsymbol{x}*\overline{\boldsymbol{v}}_{ik}=\mathrm{IFFT}\left[\mathrm{FFT}(\boldsymbol{x})\mathrm{FFT}(\overline{\boldsymbol{v}}_{ik})\right]\\ &=\mathrm{IFFT}\left[\boldsymbol{X}\cdot\overline{\boldsymbol{V}}_{ik}\right]\end{aligned} \tag{14}$$

$$\begin{aligned}\boldsymbol{r}_{\hat{\boldsymbol{x}},\hat{\boldsymbol{w}}_{ik}} &= \hat{\boldsymbol{x}}*\hat{\boldsymbol{w}}_{ik}=\mathrm{IFFT}\left[\mathrm{FFT}(\hat{\boldsymbol{x}})\mathrm{FFT}(\hat{\boldsymbol{w}}_{ik})\right]\\ &=\mathrm{IFFT}\left[\hat{\boldsymbol{X}}\hat{\boldsymbol{W}}_{ik}\right]\end{aligned} \tag{15}$$

with $*$ denoting the convolution operation, $\mathrm{FFT}(\cdot)$ and $\mathrm{IFFT}(\cdot)$ denoting the FFT and IFFT operations, respectively.

## 4 Experimental results

### 4.1 Data description

The results presented in this paper are based on measured airplane data. The parameters of the targets and radar are shown in Table 1, and the projections of target trajectories onto ground plane are shown in Fig. 2, from which the aspect angle of an airplane can be estimated according to its relative position to radar. As shown in Fig. 2, the measured data are segmented. Training samples and test samples are from different data segments, among which the 2nd and the 5th segments of Yark-42, the 5th and the 6th segments of An-26, the 6th and the 7th segments of Cessna Citation S/ II are taken as the training samples, other data segments are taken as test samples. According to Fig. 2, the elevation angles of the test samples are different from those of the training samples. Thus the generalization performance of the recognition method can be tested.

**Table 1** The parameters of planes and radar in the ISAR experiment

| Radar parameters | Center frequency<br>bandwidth | 5 520 MHz<br>400 MHz | |
|---|---|---|---|
| Planes | Length/m | Width/m | Height/m |
| Yark-42 | 36.38 | 34.88 | 9.83 |
| An-26 | 23.80 | 29.20 | 9.83 |
| Cessna Citation S/II | 14.40 | 15.90 | |

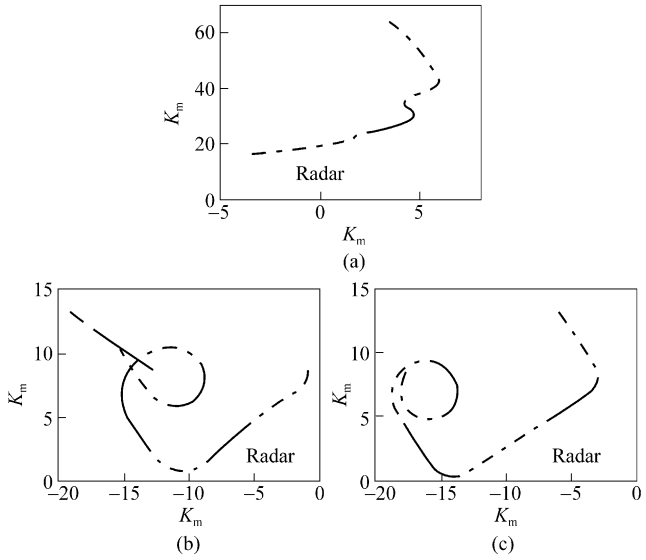


**Fig. 2** The projections of target trajectories onto ground plane. (a) Yark-42; (b) An-26; (c) Cessna Citation S/II

### 4.2 Comparison between recognition performances

The proposed weighted HRRP feature and average profile template are applied to MCC-TMM [1, 4, 6] and RBFN [6] to compare their recognition performances. Table 2 shows their confusion matrices and average recognition rates. Obviously, our new feature vector achieves better recognition performances than traditional average profile template. Especially, the recognition rates of An-26 obtained by the two classification algorithms using weighted HRRP feature are improved greatly, since An-26 is a propeller-driven aircraft and our feature extraction method can effectively reduce the effect from the unstable echoes from the propeller. In addition, the recognition rates obtained by RBFN are all larger than those by MCC-TMM. Therefore, advanced classifiers can effectively improve recognition performances.

## 5 Comparison between our method and AGC

### 5.1 Some problems existing in AGC

The main procedure of AGC is as follows [7].

1) Preprocessing: the non-Gaussian distributed data are turned into Gaussian distributed data by power transformation.

**Table 2** The confusion matrices and average recognition rates of MCC-TMM and RBFN using average profile feature and weighted HRRP feature

| Classifiers | MCC-TMM | | | | | | RBFN | | | | | |
|---|---|---|---|---|---|---|---|---|---|---|---|---|
| Feature vector | Average profile template | | | Weighted HRRP feature | | | Average profile template | | | Weighted HRRP feature | | |
| | Yark -42 | Cessna Citation S/II | An -26 | Yark -42 | Cessna Citation S/II | An -26 | Yark -42 | Cessna Citation S/II | An -26 | Yark -42 | Cessna Citation S/II | An -26 |
| Yark-42 | 81.25 | 1.00 | 14.75 | 90.25 | 0.00 | 1.50 | 76.25 | 0.50 | 10.25 | 97.50 | 0.00 | 2.75 |
| Cessna Citation S/II | 2.75 | 77.75 | 43.00 | 0.25 | 88.50 | 3.75 | 0.00 | 73.75 | 21.75 | 0.00 | 95.25 | 4.75 |
| An-26 | 16.00 | 21.25 | 42.25 | 9.50 | 11.50 | 94.75 | 23.75 | 25.75 | 68.00 | 2.50 | 4.75 | 92.50 |
| Average recognition rate/% | | 67.08 | | | 91.17 | | | 72.67 | | | 95.08 | |

2) Template database: estimate the average profile and variance profile of each HRRP frame. $\{\bar{\boldsymbol{\mu}}_{ik}, \bar{\boldsymbol{c}}_{ik} \mid i = 1,2,\cdots, C, k = 1,2,\cdots,K\}$ with $\bar{\boldsymbol{\mu}}_{ik} = \boldsymbol{\mu}_{ik} \big/ \|\boldsymbol{\mu}_{ik}\|_2$ and $\bar{\boldsymbol{c}}_{ik} = \boldsymbol{c}_{ik} \big/ \|\boldsymbol{\mu}_{ik}\|_2^2$.

3) Test phase: let $\bar{\boldsymbol{x}}_\tau$ be the power transformed, amplitude-scale normalized and time-shift compensated test HRRP sample. Then

$$d_{ik} = \ln|\bar{\boldsymbol{c}}_{ik}| + (\bar{\boldsymbol{x}}_\tau - \bar{\boldsymbol{\mu}}_{ik})^{\mathrm{T}} \sum_{ik}^{-1} (\bar{\boldsymbol{x}}_\tau - \bar{\boldsymbol{\mu}}_{ik}) \quad i = 1,2,\cdots,C,\ k = 1,2,\cdots,K \tag{16}$$

where $\sum_{ik} = \mathrm{diag}(\bar{\boldsymbol{c}}_{ik})$. If

$$j = \arg\min_i (\min_k d_{ik}), \quad i = 1,2,\cdots,C,\ k = 1,2,\cdots,K \tag{17}$$

$\boldsymbol{x}$ belongs to target $T_j$.

Because using variance matrix of target HRRP can reflect their amplitude fluctuation property, AGC outperforms MCC-TMM in radar HRRP target recognition. However, the preprocessed data are assumed to follow Gaussian distribution in AGC. If test data mismatch with the distribution model estimated from training data or the parameters of distribution model are not estimated exactly, the recognition performance of AGC will degrade. Firstly, the sample number of an HRRP frame is not large in radar HRRP target recognition, therefore the estimated average profile and variance profile must have the estimation errors. Secondly, as discussed in Sect. 3.1, due to the amplitude-scale sensitivity, the target-aspect templates and the test data should be amplitude-scale normalized (e.g., $L_2$ normalization) before matching. As described above, the $L_2$ normalization is also applied to AGC. AGC assumes that the test data and the training data in the matched HRRP frame should follow same distribution. Nevertheless, since range cells of an HRRP have different amplitude fluctuation properties, $L_2$ normalization, which makes the energy of a vector equal to one, may change the data's distribution model, and consequently the originally matched test data and template maybe become mismatched after $L_2$ normalization. This can be explained by an example shown in Fig. 3, which also comes from the measured data of "Yark-42". Fig. 3(a) shows two raw HRRP samples in an HRRP frame, which have similar waveforms except for the echoes in one range cell. However, after amplitude-scale normalization, as shown in Fig. 3(b), their waveforms are quite different. Thus the variance profiles estimated from the raw HRRP frame and the amplitude-scale normalized HRRP frame are also different as shown in Fig. 3(c). Therefore, the $L_2$ normalization may cause the test data to mismatch with the distribution model estimated from training data. Fig. 3(d) shows the corresponding weighted HRRP feature vectors. Compared with the raw HRRP samples and the amplitude-scaled normalized samples, our weighted HRRP feature vectors are more stable.

Our feature extraction method differs from AGC in that there is no distribution assumption or parameter estimation for target HRRP. In our method, based on scattering center model, HRRP components are multiplied by different weights, which depend on the corresponding average profile and variance profile. Thus, the weighted HRRP feature can represent the scatterer distribution in every range cell.

## 5.2 Recognition results of AGC

Table 3 shows the recognition results of AGC. Compared with Table 2, the average recognition rate obtained by MCC-TMM using our new feature vector is approximately 6 percentage points larger than that obtained by AGC. Especially, the misclassified samples of Cessna Citation S/II and An-26 in MCC-TMM using weighted HRRP feature decreases greatly. As shown in Fig. 2, compared with Yark-42, the course and elevation angles of Cessna Citation S/II and An-26 change much more, thereby their HRRP samples are relatively unstable. Thus, the improvement in the recognition performances of Cessna Citation S/II and An-26 demonstrates that our weighted HRRP feature can describe the scattering property of the target better.

**Table 3** The confusion matrix and average recognition rate of AGC

| | Yark-42 | Cessna Citation S/II | An-26 |
|---|---|---|---|
| Yark-42 | 93.50 | 1.25 | 3.50 |
| Cessna Citation S/II | 0.00 | 69.00 | 2.75 |
| An-26 | 6.50 | 29.75 | 93.75 |
| Average recognition rate/ % | | 85.42 | |

## 6 Conclusions

The average profile can represent the scatterer strength information of all range cells, and the variance profile can represent the scatterer distribution information of all range cells. The weighted HRRP feature extracted by our feature extraction method, which effectively fuses the average profile with the variance profile of an HRRP frame, can describe the scattering property of a target better. Furthermore, a fast joint amplitude-shift matching algorithm is proposed in this paper, by which the weighted HRRP feature can be used in any classifier based on Euclidean distance with greatly-reduced computation burden. The experimental results based on measured data show that the new feature extraction method can improve recognition performances greatly.

**Acknowledgements** This study was partially supported by the National Science Foundation of China (No. 60302009) and the National Defense Preresearch Foundation of China (No. 41307501).

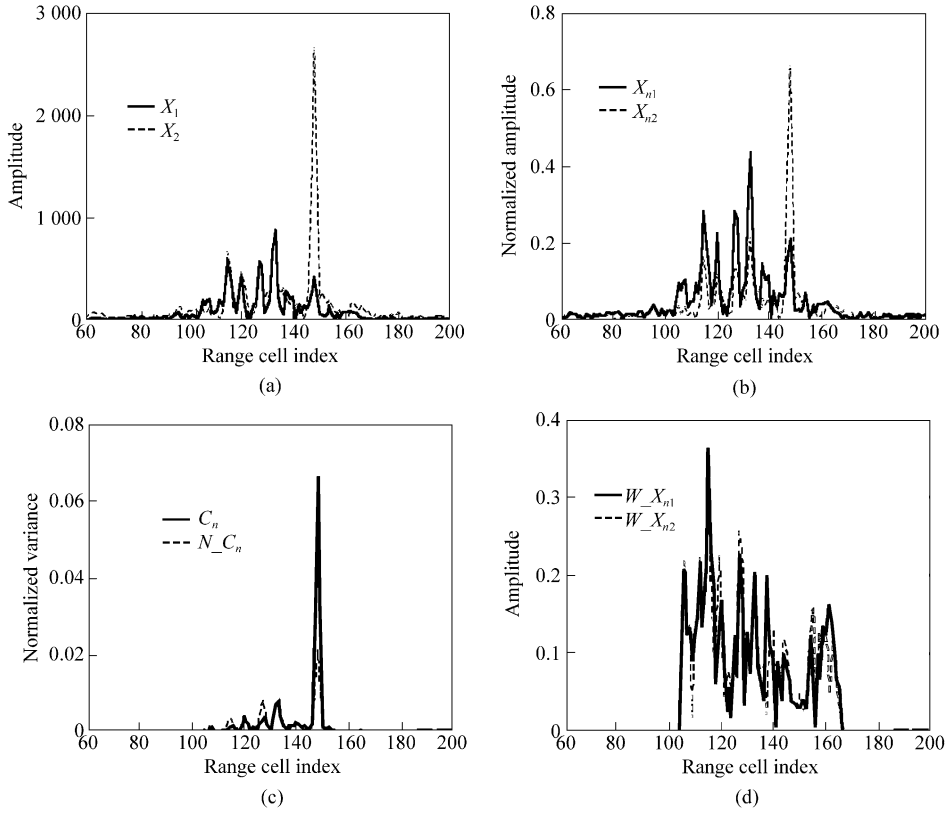


**Fig. 3** An example of distribution mismatch in an HRRP frame of "Yark-42". (a) Two raw HRRP samples in an HRRP frame; (b) The amplitute-scale normalized samples; (c) The variance profiles estimated from the raw HRRP frame and the amplitude-scale normalized HRRP frame; (d) The weighted HRRP feature vectors

## References

1. Li H-J., Yang S.-H.., Using range profiles as features vectors to identify aerospace objects, IEEE Trans. Adv. Packaging, 1993, 41(3): 261–268
2. Xing M. D., Bao Z., Pei B. N., The properties of high-resolution range profiles, Opt. Eng., 2002, 41 (2): 493–504
3. Du L., Bao Z., Xing M. D., Research on the characteristics of the radar one dimension range profile of the aircraft target, Journal of Xidian University., 2001, 28(Sup.): 14–19 (in Chinese)
4. Liu H. W., Du L., Yuan L., Bao Z., Progress in radar automatic target recognition based on high range resolution profile, Journal of Electronics & Information Technology, 2005, 27(8): 1328–1334 (in Chinese)
5. Liao X. J., Bao Z., Xing M. D., On the aspect sensitivity of high resolution range profiles and its reduction methods, the Record of the IEEE 2000 International Radar Conference., Alexandria, May 2000, 310–315
6. Du L., Liu H. W., Bao Z., Radar HRRP target recognition based on higher order spectra, IEEE Trans. S. P., 2005, 53(7): 2,359–2368
7. Jacobs S. P., O'sollivan J. A., Automatic Target Recognition Using High-Resolution Radar Range Profiles,Washington: Washington University, 1999
8. Steinberg B. D., Microwave Imaging with Large Antenna Arrays: Radio Camera Principle and Technique, New York: John Wiley and Sons, 1983
9. Ye W., Study of the Inverse Synthetic Aperture Radar Imaging and Motion Compensation, Xi'an: Xidian University, 1996